Laser ablation based technique for flexible fabrication of microlenses in polymer materials.

Kris Naessens, Peter Van Daele and Roel Baets.

Universiteit Gent / IMEC – Dept. of Information Technology (INTEC)
Sint-Pietersnieuwstraat 41, B-9000 Gent, Belgium.
E-mail: kris.naessens@intec.rug.ac.be.
http://www.intec.rug.ac.be/groupsites/opto/ocs/

Laser ablation is a versatile technique for fabricating microstructures on polymer surfaces. Due to the nature of the process, the fabrication of the microstructure can take place in a very late stage of a heterogeneous assembly. This makes laser ablation very attractive for fabricating micro-optical components on opto-electronic assemblies in comparison to other fabrication techniques like injection molding and embossing.
In this paper we will report on the first experimental results of microlens fabrication with excimer laser ablation techniques. By scanning the polymer surface along multiple circular paths with a circular beam of a pulsed excimer laser, one is able to obtain a lens shape with arbitrary focal distance and diameter. Important issues such as the choice of ablation parameters, the selection of scanning path and the performance of the resulting laser ablated lens will be discussed.

Keywords: laser ablation, microstructures, microlenses.

1. Introduction.

One of the main trends in current opto-electronic device fabrication, is a continual miniaturization of the components in order to minimize material and manufacturing costs and maximize speed. This tendency has been the main drive to develop micro-optics into a full fledged discipline. In every application which requires manipulation, imaging and/or focussing of light beams and which does not allow the insertion of macro-optic components due to lack of space, micro-optical solutions have to be developed. This is particularly the case in manipulation of one-dimensional or two-dimensional arrays of optical beams.
A number of fabrication technologies for micro-optical components are at our disposal: on mass replication level embossing and injection molding are widely used. For prototyping or small quantities, micro-electronic based technologies like lithography, laser- and e-beam writing, deep-proton lithography, micro-jet printing, LIGA and even laser-ablation can be applied.
In literature, excimer laser ablation has been reported as a viable technology to realize micro-optical components. In general, complex mask patterns for fabrication of Fresnel[1] or refractive microlenses[2] are required for direct ablation techniques while other methods involve the use of selected polymer materials in a process based on ablation and subsequential thermal reflow[3] or annealing[4], or irradiation of doped polymers[5], in which precise control of focal length can be difficult.

The approach we propose here is based on direct ablation using one circular aperture for shaping the microlens and another larger aperture for cleaning and smoothing of the machined surface. All laser parameters remain constant during fabrication, no complex and/or moveable masks are used and no diffusion processes are involved. The shape of the lens is solely determined by the circular movements of the translation stage on which the sample is placed and is not restricted to any particular circular symmetric shape.
Time of fabrication varies from less than one minute to several minutes for a single microlens. Since the circular aperture can be repeated on one single mask, fabrication time for a 2D array of identical lenses remains the same as long as the full array fits within the field of the projection lens of the ablation system.
The whole fabrication process is an essentially non-contact method and can be performed on a multitude of polymer materials, including polymer layers deposited on semi-conductor material. It can therefore be easily applied in a final fabrication step of an opto-electronic heterogeneous assembly.

2. Microlens fabrication approach.

The lens fabrication method as described below uses a simple circular hole as beam aperture for the excimer laser and a high precision translation stage (1 μm resolution) carrying the polymer substrate, capable of making circular movements by interpolation. The pulse energy and the pulse frequency (number of pulses per second, f) of the laser

remain constant during the process. While the excimer laser is firing pulses, the translation stage makes subsequent circular concentric movements with different radii and speeds. By careful choice of both speed and radius, one can obtain an arbitrary desired surface shape with circular symmetry, as we will explain below.

2.1. Profile of the ablated trench.

In the experimental set-up we use a projection lens to image the circular aperture onto a polymer substrate with a certain demagnification. We assume that this aperture is homogeneously irradiated by the laser beam, resulting in a constant energy density on the polymer surface within the image area (diameter ρ). A circular movement of the table will result in the ablation of a closed trench. If R is the radius of the circle, v the speed of the table movement and dpp the ablation depth per pulse, the resulting ablated profile can be described as

$$\text{Depth}(s, R, v) = \text{Prob}(s, R, v) \cdot A(r, v)$$

in which

$$\text{Prob}(s, R, v) = \frac{1}{\pi} \cdot \text{acos}(\theta) \cdot \Phi(R + \frac{\rho}{2} - |s|) \cdot \Phi(\frac{\rho}{2} - R + |s|) \cdot$$

$$\Phi(R - \frac{\rho}{2} + |s|) + \Phi(\frac{\rho}{2} - R + s) \cdot \Phi(\frac{\rho}{2} - R - s) \cdot \Phi(\frac{\rho}{2} - R)$$

$$A(r, v) = \frac{2 \cdot \pi \cdot R \cdot f \cdot dpp}{v}$$

Φ is defined by $\Phi(x) = \begin{cases} 0 & x < 0 \\ 1 & x > 0 \end{cases}$ (heaviside function) and

$$\theta = \frac{(\frac{\rho}{4}^2 - R^2) - s^2}{-2 \cdot R \cdot |s|}$$

with s the coordinate along the vertical axis.

Prob(s,R,v) can be interpreted as the normalized probability of a point with coordinate s, to be illuminated by the laser beam during one circular move of the sample stage (FIG. 1). One can distinguish two contributions to calculate this probability: the first one takes care of the area that is continuously exposed to the laser pulses during the table movement and for which prob(s,R,v) is thus equal to 1. The second contribution is valid for points that are only partially illuminated during one circular movement of the table. This value can be obtained by calculating the overlap of the circle C1 and the aperture. A(r,v) represents the full ablation depth for points with prob(s,R,v) equal to 1.

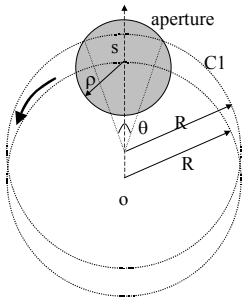

FIG. 1: Definition of the geometrical parameters in the expression of the trench profile.

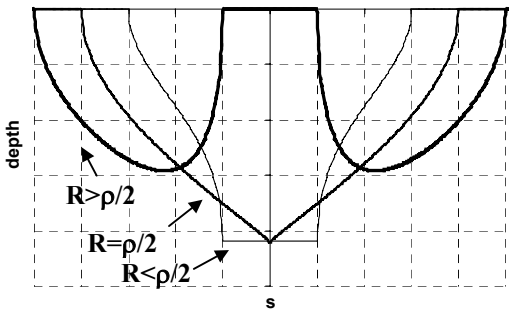

FIG. 2: Profile of the ablated trench as function of R and ρ.

In FIG. 2 the upper function is illustrated for several values of R and ρ. Note the different scaling for the depth and coordinate axis. A comparison between this calculated profile and the experimental result for one value of R and ρ is shown in FIG.3.

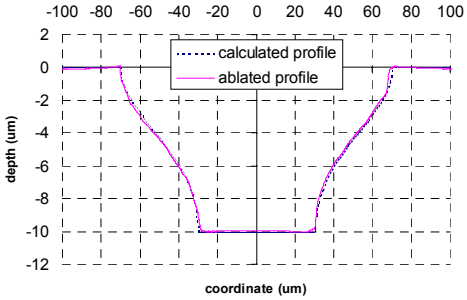

FIG. 3: Calculated and experimental profile of a circular trench (ρ = 100 μm) with R = 20 μm and v = 20 μm/s.

2.2. Approximation of the desired lens shape.

In a next step we assume that a microlens shape can be approximated by having the substrate make several of the circular paths mentioned above with different radii and at variable speeds while the laser is firing pulses. This idea is illustrated in FIG. 4.

The overlap of the subsequent pulses within one circle determines the depth per channel and the overlap between the neighbouring channels can be chosen to achieve a smooth surface in accordance with the intended shape.

A least square method has been applied to optimize the radii and stage velocity in order to approximate a desired profile. The algorithm produces an approximation in a very fast way, however it should be noted that it is still based on finding a local and not an absolute minimum.

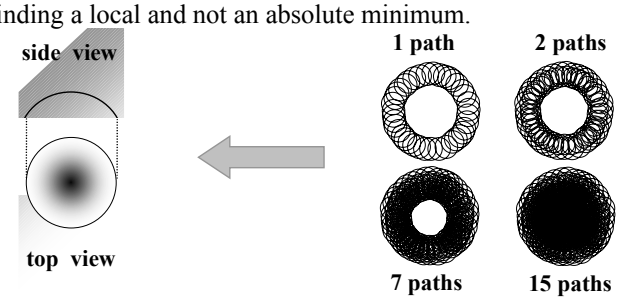

FIG. 4: Approximation of a curved surface by subsequent ablation of circular trenches.

2.3. Laser ablation of the microlens.

In a last stage, the optimal radii and speeds are used as an input to generate the control code for the translation stage of the laser ablation unit. This code will split up trenches with a depth larger than a certain d_{max} in several trenches with the same radii but smaller depths (higher speed of movement). And the order in which the several circles are written, as well as the starting coordinates for every circle can be randomized.

Finally the code is executed in order to ablate the desired surface shape. During the ablation process, laser pulse energy and frequency are kept constant. Only one aperture, which is imaged onto the polymer surface, is required and refocusing of the beam during the process is not necessary.

3. Experimental results and discussion.

The experiments were carried out with a Lumonics Pulse Master 848 (ArF 193 nm wavelength) and by means of an optical set-up (Micromaster from Optec) as in FIG 5. Until now, our research has been focused on polycarbonate as substrate material. In the near future however, other polymer materials will be investigated.

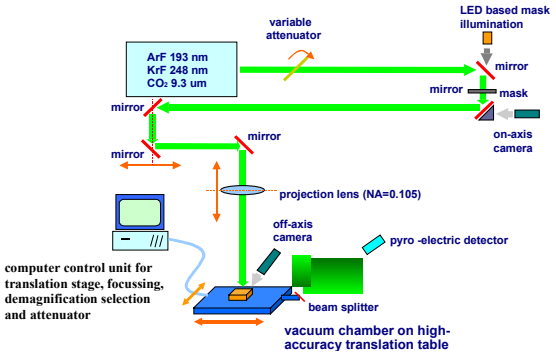

FIG. 5 : Laser ablation set-up.

A Molectron J3 pyroelectric joulemeter, put at far distance from the image plane, was used for energy density measurements (by aiming the beam at the beamsplitter). The polymer sample is about 250 µm thick and is positioned in a flow chamber mounted on the translation stage (FIG. 6). The ablated patterns and profiles have been measured by means of a confocal microscope of BMT.

In FIG. 7 an example is given in which an approximation of a cone with a half-top angle of 70 degrees is calculated. The beam aperture had an on-substrate imaged diameter of 100 µm with an energy density of 180 mJ/cm^2.

Note that laser ablation can only take away material from the substrate. This means that the top of the desired profile still needs to be below the surface level of the substrate (depth = 0in FIG. 7) and thus the structure has to be buried into the material. Measurement of the ablated sidewalls reveal a R_t (root mean square roughness) of less than 40 nm. Similar results have been achieved for other angles, including horizontal surfaces, buried into the substrate.

The same technique has been applied to fabricate a micro-lens with a diameter of 200 µm and a target focal length of 340 µm). FIG. 8 shows the 3D image of the result: an ablated microlens with a diameter of 200 µm and a focal length of 353 µm (radius of curvature = 208 µm, n_{pc} = 1.59, NA ≅ 0.28). The approximation was accomplished by using 25 circles of different radii (FIG. 8, left) with an aperture of 100 µm. The profile of the lens is given in FIG. 9. and FIG. 10 illustrates the imaging qualities. The slight deviation in curvature of the ablated lens is not yet fully understood and still has to be determined, but is likely caused by a slightly smaller beam aperture.

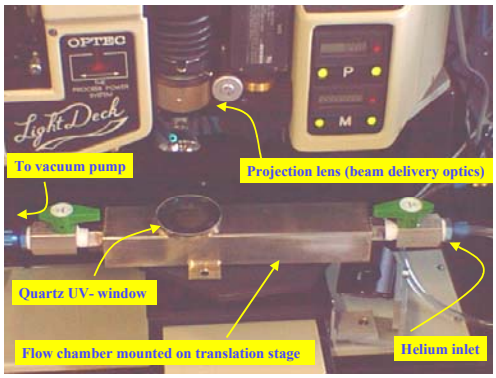

FIG.6: Detail of the flow chamber.

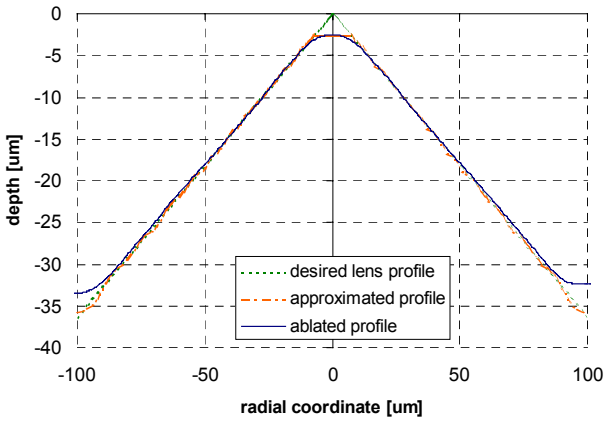

FIG. 7: Desired, approximated and ablated profile (E = 180 mJ/cm^2 at 20 Hz operation).

After ablation of the profile, the sample is post-processed by additional exposure of the ablated zone by an aperture (diameter ρ_{pp}) covering an area larger than the full lens surface, and at the same energy density as the previous fabrication step. During the exposure, the table performs a circular move with a small radius r_{pp} in order to ensure a homogeneous exposure within the region with diameter ρ_{pp} - $2 \cdot r_{pp}$. Since no homogenizer is used in our set-up, this proves to be a useful way to spatially average the optical power within the aperture.

This post-processing accomplishes an ultimate debris removal. Another benefit of the post-illumination of the sample is masking the possible creation of a ripple due to

the not perfectly smooth overlap between the several ablated channels and to the discrete nature of the ablation process.

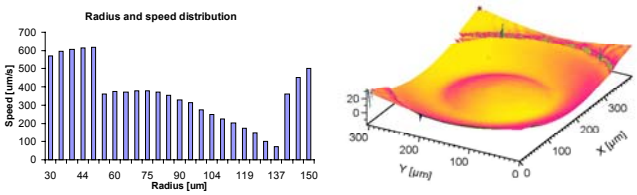

FIG. 8: Distribution of radii and contour speeds (left). Profile of the desired and approximated microlens (right).

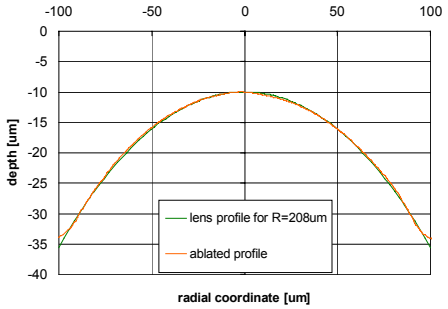

FIG. 9: Profile of the ablated microlens.

The origin of the latter type of ripple can be explained as follows: when the rotational move of the table is slow enough, the subsequent pulses will hit the sample in practically the same area. If those regions only differ about Δ in distance, then we can assume that there is no ripple when Δ is small enough so the lens can not resolve it ($\Delta <$ 1.6 μm in the image plane). This limit can be translated in a maximum velocity of the table. The influence of this upper limit can be observed in FIG. 7: at the top of the cone (near depth = 0), the calculated profile can not approximate the desired one accurately and becomes rounded.

On the other hand, we do not like to write the trenches to full depth in one go since this can heavily influence the ablation of a neighbouring, overlapping channel. Therefore, a maximum depth is determined which is allowed to be ablated in one go. This results in a minimum velocity of the table. Both speed limits can be rather close to each other in practice. The minimum value is easy to implement in the generation of control code for the laser ablation process by simply chopping deep trenches in several channels with a much smaller depth and thus fabricated at higher speeds. Handling the maximum value however is not that evident: given a certain aperture and a required depth, it is very much possible that the table has to move faster than allowed by Δ. This is in particular the case when using large apertures and requiring small depths. To a certain extent we can solve this problem by limiting the pulse energy and/or introducing an offset in depth (bury the microlens deeper into the polymer sample). However, we observed that post-processing of the sample tends to flatten out that ripple as well. This means that a higher maximum velocity limit can be used than defined by the projection lens.

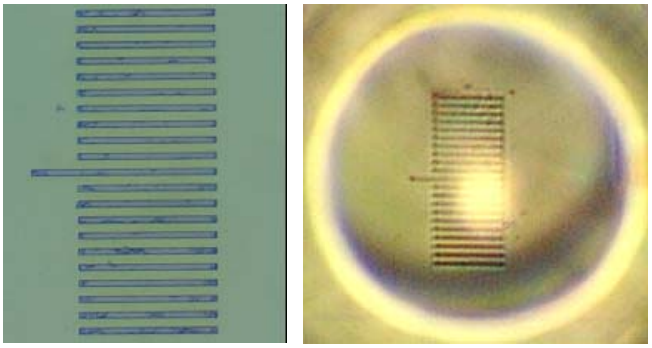

FIG. 10: Imaging properties of the ablated microlens. Test pattern (left), virtual image (right).

Conclusions.

We implemented a method to ablate circular symmetric structures, more in particular microlenses, using a very simple laser ablation set-up. The first results are very encouraging in terms of approximation quality of the desired profile and surface roughness.

Due to the flexibility of the process in terms of diameter and focal length of the ablated microlenses, this technology is very suitable for fast fabrication on prototyping level. In particular, due to the non-contact nature of excimer laser ablation, the process can be very easily applied for optical surface shaping in a very late stage of an opto-electronic heterogeneous assembly.

Further research is now focused on analysis and evaluation of the surface in terms of optical quality and performance of the lenses in an optical set-up.

Acknowledgements.

This work has been performed within the framework of the Flemish IWT project ITA-II "VLSI photonics" and the Belgian IUAP-13 project. We would like to thank Thermo Scientific B.V., Breda, the Netherlands, for making the confocal microscopy set-up of BMT available to us.

References.

[1] X. Wang, J.R. Leger and R.H. Prediker, "Rapid fabrication of diffractive optical elements by use of image-based excimer laser ablation", Appl. Opt. Vol. 36 No. 20, p4660-4665, 1997.

[2] R. Matz, H. Weber, G. Weimann, "Laser-induced dry etching of integrated InP microlenses", Appl. Phys. A Vol. 65, p349-353, 1997.

[3] Stephen Mihailov and Sylvain Lazare, "Fabrication of refractive microlens arrays by excimer laser ablation of amorphous Teflon", Appl. Opt. Vol. 32 No. 31, p6211-6218, 1993.

[4] M. Wakaki, Y. Komachi and G. Kanai, "Microlenses and microlens arrays formed on a glass plate by use of a CO^2 laser", Appl. Opt. Vol. 37 No. 4, p627-631, 1998

[5] F. Beinhorn , J. Ihlemann , K. Luther , J. Troe , "Micro-lens arrays generated by UV laser irradiation of doped PMMA", Vol. 68 No. 6, p709-713.